

Incorporating Unlabelled Data into Bayesian Neural Networks

Mrinank Sharma¹ Tom Rainforth¹ Yee Whye Teh¹ Vincent Fortuin^{2,3}

Abstract

We develop a contrastive framework for learning better prior distributions for Bayesian Neural Networks (BNNs) using unlabelled data. With this framework, we propose a practical BNN algorithm that offers the label-efficiency of self-supervised learning and the principled uncertainty estimates of Bayesian methods. Finally, we demonstrate the advantages of our approach for data-efficient learning in semi-supervised and low-budget active learning problems.

1. Introduction

Bayesian Neural Networks (BNNs) are powerful probabilistic models that combine the flexibility of deep neural networks with the theoretical underpinning of Bayesian methods (Mackay, 1992; Neal, 1995). Indeed, by placing prior distributions over their weights and biases and performing posterior inference, BNNs promise several benefits, such as principled uncertainty quantification (Wilson & Izmailov, 2020) and data-efficient learning (Gal et al., 2017).

Despite their promise, several concerns have been raised with BNN priors (Wenzel et al., 2020; Izmailov et al., 2021a), igniting an interest in improving the prior (Nalisnick, 2018; Tran et al., 2020; Fortuin, 2022). One hopes that better BNN priors, in turn, lead to improved generalisation and label-efficiency (Williams & Rasmussen, 2006).

In this work, we aim to improve the priors and performance of BNNs by leveraging unlabelled data to better specify prior predictive distributions.

To do so, we take inspiration from the contrastive learning literature (Chen et al., 2020a; Oord et al., 2019; Chen & He, 2020; Grill et al., 2020; He et al., 2020). Rather than specifying our prior beliefs directly over network weights or predictive functions, we reason using *data* and *data transformations* that preserve semantic information (§3.1). Specifically, we create labelled contrastive task datasets using

unlabelled data, which *themselves* reflect a belief that augmented examples are more likely to have the same label on the downstream task than randomly sampled pairs of images. We then use parameter-sharing to create a link between the labels of the downstream and contrastive task datasets, allowing the unlabelled data to be leveraged for improved downstream predictions.

Using this framework, we develop a practical BNN algorithm that we call *Bayesian Self-Supervised Learning* (BSSL; §3.2). Like self-supervised learning algorithms, our approach has two steps. We first maximise a lower bound of a log-marginal likelihood computed using only unlabelled data. Following this, we perform approximate inference on task-specific parameters to make downstream predictions.

On empirical evaluations, we find that our resultant algorithm offers both the label-efficiency of self-supervised learning and principled uncertainty estimates of Bayesian methods (§4). Indeed, we find BSSL to be more label-efficient than BNNs, in line with the expectation that the BSSL prior predictive is better suited to downstream tasks than standard BNN priors. Moreover, BSSL is better calibrated than SimCLR (Chen et al., 2020a), a popular contrastive learning algorithm.

To investigate the hypothesis that the improved predictive performance of BSSL is due to the learnt prior predictive distribution, we develop methodology that quantifies the suitability of the prior predictive *itself* (§5). Indeed, we find the BSSL prior is more suitable than common BNN priors.

Finally, we demonstrate the advantages of our BSSL framework for data-efficient learning on semi-supervised and low-budget active learning problems (§6).

Overall, we show that BSSL is a competitive and principled alternative to conventional BNNs. Contrastive pre-training offers an effective mechanism for learning a suitable prior predictive distribution from unlabelled data. Combining this with approximate Bayesian inference of task parameters yields practical and performant Bayesian deep learning algorithms. To summarise, our key contributions are:

- We develop a contrastive framework for Bayesian Self-Supervised Learning (BSSL), which allows probabilistic discriminative models to leverage large quantities of unlabelled data for improved performance.

¹University of Oxford ²University of Cambridge
³Helmholtz AI, Munich. Correspondence to: Mrinank Sharma
<mrinank.sharma@eng.ox.ac.uk>.

- Using this framework, we introduce a practical BNN algorithm that offers the sample-efficiency of self-supervised learning and the principled, well-calibrated uncertainty estimates of Bayesian methods.
- We develop new methodology to assess prior predictive distributions and show the success of BSSL can, at least in part, be attributed to its learnt prior predictives. Conversely, common BNN prior predictives are not well suited for downstream tasks.
- Finally, we demonstrate that BSSL supports label-efficient learning in semi-supervised and low-budget active learning settings.

2. Background

Bayesian Neural Networks Let $f_\theta(x)$ be a deep neural network with parameters θ and $\mathcal{D} = \{(x_i, y_i)\}_i$ be an observed dataset on which we want to predict y from x . A Bayesian Neural Network (BNN) specifies a prior over network parameters, $p(\theta)$, as well as a likelihood, $p(y|f_\theta(x))$, which in turn define a posterior distribution $p(\theta|\mathcal{D}) \propto p(\theta) \prod_i p(y_i|f_\theta(x_i))$. To make predictions, we use the posterior predictive $p(y|x, \mathcal{D}) = \mathbb{E}_{p(\theta|\mathcal{D})}[p(y|f_\theta(x))]$.

Since exact inference is intractable for neural networks, practitioners use approximate inference algorithms. Some approaches sample from the posterior (Neal, 1995; Welling & Teh, 2011), while others learn an approximate posterior (Mackay, 1992; Blundell et al., 2015; Daxberger et al., 2021; Kingma et al., 2015; Maddox et al., 2019). Further, deep ensembles are an effective approach for uncertainty quantification (Lakshminarayanan et al., 2017; Ovadia et al., 2019), and have been cast as approximate inference (Wilson & Izmailov, 2020; D’Angelo & Fortuin, 2021).

Contrastive Learning Contrastive learning is a popular approach for self-supervised learning (Chen et al., 2020b;a; Grill et al., 2020; Hénaff et al., 2020; Oord et al., 2019; Chen & He, 2020). Self-supervised learning algorithms use large quantities of unlabelled data to generate auxiliary, supervised learning tasks that are used for unsupervised pre-training. Following this, the pre-trained network is fine-tuned on the task of interest, known as the downstream task. Contrastive learning approaches in particular maximise the agreement between representations of augmented views of an input datum, whilst also maximising the disagreement of representations of different points.

3. A Contrastive Framework for Bayesian Self-Supervised Learning

Although BNNs are principled probabilistic models (Mackay, 1992; Neal, 1995), they cannot leverage unlabelled data to boost their performance, in contrast to self-

supervised learning algorithms. Therefore, it is natural to wonder: is it possible to combine the benefits of Bayesian methods and self-supervised learning.

Problem Specification Suppose $\mathcal{D}^u = \{x_i\}_i$ is an unlabelled dataset of examples $x_i \in \mathbb{R}^n$ with $x_i \sim P_{\mathcal{D}}$, where $P_{\mathcal{D}}$ is the underlying data distribution. Let $\mathcal{D}^t = \{(x_i, y_i)\}_i$ be a labelled dataset corresponding to a supervised task of interest. y_i is the target associated with x_i and could be, e.g., a class label. We want to exploit \mathcal{D}^u to help us solve this downstream task of interest.

For conventional, discriminative BNNs, \mathcal{D}^u provides no evidence about the BNN’s weights (§2). In other words, for a standard BNN, we have $p(\theta|\mathcal{D}^u, \mathcal{D}^t) = p(\theta|\mathcal{D}^t)$, rendering the BNN unable to leverage the unlabelled dataset to improve performance. As such, a BNN is reliant on having a prior $p(\theta)$ that is well-suited for \mathcal{D}^t . Unfortunately, recent work has raised several concerns with the priors used for BNNs (Wenzel et al., 2020). Indeed, we later confirm (§5) that standard BNN priors are not well suited to the tasks they are used on. We, therefore, aim to use \mathcal{D}^u to improve the prior used for \mathcal{D}^t .

3.1. A Contrastive Framework for Bayesian Self-Supervised Learning

To make inroads on leveraging \mathcal{D}^u for improved BNN prior predictives, we use the following key insight: we can specify our prior beliefs using *data* and *data transformations* that preserve semantic information. Intuitively, randomly sampled images are unlikely to be semantically consistent with one another, and thus unlikely to have the same label on a downstream task. In contrast, augmented images are likely to be consistent as the augmentations we use are designed to maintain semantic content. We can use this insight to generate labelled, *self-supervised* task datasets that reflect the prior beliefs encoded through the chosen data transformations and data distribution. These datasets can then be conditioned on when making predictions.

Concretely, we have a set of data augmentations $\mathcal{T} = \{t : \mathbb{R}^n \rightarrow \mathbb{R}^n\}$ that preserve semantic content. We use \mathcal{T} to encode our prior beliefs that are transferred to a labelled *contrastive task dataset*, \mathcal{D}^c , as follows:

1. Draw a minibatch of size M points from \mathcal{D}^u , $\{x_i\}_{i=1}^M$.
2. Sample $t^A, t^B \sim \mathcal{T}$ and augment each x_i twice, yielding \tilde{x}_i^A and \tilde{x}_i^B .
3. Form \mathcal{D}^c by assigning \tilde{x}_i^A and \tilde{x}_i^B the same class label.

We therefore have $\mathcal{D}^c = \{(\tilde{x}_i^A, i)\}_{i=1}^M \cup \{(\tilde{x}_i^B, i)\}_{i=1}^M$. In words, \mathcal{D}^c is an M -class classification problem, where we want to predict the source image index corresponding to each augmented image. We can repeat this process and create a large set of contrastive task datasets, $\{\mathcal{D}_j^c\}$, using

the large unlabelled dataset, \mathcal{D}^u . Since the augmentation schemes in \mathcal{T} preserve semantic information, and because different source images are unlikely to be semantically similar and *could* have different labels on the downstream task, the contrastive task datasets themselves thus capture our prior beliefs about downstream labels.

We have used \mathcal{D}^u to generate a set of labelled datasets. But, one would typically use a separate discriminative model (like a BNN) for each $\{\mathcal{D}_j^c\}$ and \mathcal{D}^t , which renders the labels of \mathcal{D}_j^c and \mathcal{D}^t independent of one other. But, to be able to leverage the contrastive task data for downstream predictions, we need the labels of \mathcal{D}_j^c to inform the labels of \mathcal{D}^t somehow.

To create this link, we employ parameter sharing. We assume the labels for both \mathcal{D}_j^c and \mathcal{D}^t are generated using likelihood $p(y^t|x, \theta^s, \theta^t)$ where θ^s is shared across the tasks $\{\mathcal{D}_j^c\}$ as well as \mathcal{D}^t (see Fig. 1). Each dataset has a different θ^t ; we use θ_j^c to denote the parameters corresponding to \mathcal{D}_j^c and θ^t to denote the parameters corresponding to \mathcal{D}^t . For a BNN, θ^s and θ^t would be the parameters of a neural network. Following the Bayesian paradigm, we then place priors over each θ^t and θ^s and make predictions using the posterior predictive:

$$\begin{aligned} p(y_\star^t|x_\star, \{\mathcal{D}_j^c\}, \mathcal{D}^t) \\ = \mathbb{E}_{p(\theta^s|\{\mathcal{D}_j^c\}, \mathcal{D}^t)}[\mathbb{E}_{p(\theta^t|\theta^s, \mathcal{D}^t)}[p(y_\star^t|x_\star, \theta^s, \theta^t)]], \end{aligned} \quad (1)$$

where we have used that the downstream task parameters θ^t are independent of $\{\mathcal{D}_j^c\}$ given the shared parameters θ^s .

To summarise, we utilise \mathcal{D}^u to help solve \mathcal{D}^t by generating self-supervised, labelled datasets $\{\mathcal{D}_j^c\}$. Because we employ parameter sharing, the labels of $\{\mathcal{D}_j^c\}$ provide information about the downstream task. As standard, we then make predictions by conditioning on all observed data, which in this case is the generated contrastive task data and the downstream task data.

To gain insight, note we predict using $p(\theta^s|\{\mathcal{D}_j^c\}, \mathcal{D}^t) \propto p(\theta^s|\{\mathcal{D}_j^c\}) \cdot p(\mathcal{D}^t|\theta^s)$ in Eq. (1). However, one would conventionally use $p(\theta^s|\mathcal{D}^t) \propto p(\theta^s)p(\mathcal{D}^t|\theta^s)$. For BNNs, θ^s and θ^t are network parameters and we see that our framework replaces the conventional BNN prior $p(\theta^s)$ with a version updated on $\{\mathcal{D}_j^c\}$ when making predictions on the downstream task. Since the contrastive task datasets were constructed to reflect our beliefs about the downstream task labels, we expect this conditioning to be helpful and indeed, we later show this to be the case (§5).

3.2. Practical Bayesian Self-Supervised Learning

Our framework allows a discriminative probabilistic model to leverage unlabelled data for data-efficient learning through parameter-sharing and self-supervision. However,

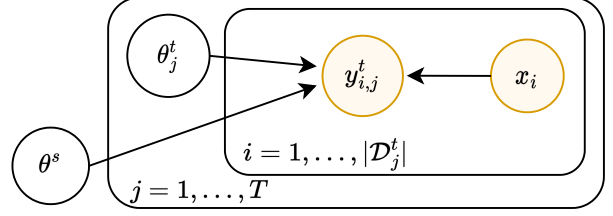


Figure 1: **Probabilistic Model for Bayesian Self-Supervised Learning.** We share parameters between different tasks, which allows us to condition on generated self-supervised data when making predictions on a new task. j indexes tasks and i indexes data points.

evaluating the posterior predictive distribution (Eq. 1) is intractable (Izmailov et al., 2021b; Sharma et al., 2022). We now develop a practical algorithm for Bayesian Self-Supervised Learning (BSSL).

Preliminaries We focus on image-classification problems. We use an encoder network that maps images to representations, and share this encoder across the contrastive task and the downstream task. The shared parameters θ^s thus correspond to the parameters of this *base encoder* $f_{\theta^s}(\cdot)$, and we normalise the representations produced by this encoder. For the contrastive task datasets and the downstream dataset, we use a task-specific linear readout layer. That is, we have $\theta_j^t = \{W_j^t, b_j^t\}$, where the subscript j indexes the task (and the same for θ_j^c). We then have $y_{i,j}^t \sim \text{softmax}(W_j^t f_{\theta^s}(x_i) + b_j^t)$, meaning that the rows of W_j^t can be understood as class templates for task j . We place a prior over θ^s and each θ_j^t .

Learning θ^s Although we could learn a distribution over the parameters of the base encoder, we can generate arbitrarily many contrastive task datasets. Since we expect the uncertainty in θ^s to vanish given enough data, we learn a point estimate for θ^s : $p(\theta^s|\{\mathcal{D}_j^c\}, \mathcal{D}^t) \simeq p(\theta^s|\{\mathcal{D}_j^c\}) \simeq \delta(\theta^s - \theta_\star^s)$, where we have also dropped the conditioning on \mathcal{D}^t , which assumes the task data contributes relatively little evidence as compared to the contrastive task datasets.

Ideally, we would set θ_\star^s using maximum-a-posteriori estimation, but evaluating the log-posterior density $\log p(\theta^s|\{\mathcal{D}_j^c\}) = \log p(\theta^s) + \sum_i \log p(\mathcal{D}_j^c|\theta^s)$ would require integrating over θ_j^c , the task-specific linear readout parameters corresponding to each \mathcal{D}_j^c . We instead use:

$$\mathbb{E}_{q(\theta_j^c)}[\log p(\mathcal{D}_j^c|\theta^s, \theta_j^c)] - D_{\text{KL}}(q(\theta_j^c)||p(\theta^c)), \quad (2)$$

which lower bounds each $\log p(\mathcal{D}_j^c|\theta^s)$ term. Eq. (2) is the evidence lower bound and $q(\theta_j^c)$ is a variational distribution over the contrastive task-specific linear readout parameters.

To learn θ^s , we thus need an appropriate variational dis-

tribution for each θ_j^c , which represents the linear readout parameters used for contrastive task \mathcal{D}_j^c . Although we could parameterise $q_\phi(\theta_j^c)$ with ϕ and learn ϕ , we would need to do this for each and every \mathcal{D}_j^c , which is inefficient.

Instead, we exploit the structure of the contrastive task, which is to predict the source image index from a set of augmented images. Recall that the base encoder produces a normalised representation for each image. We want to introduce a variational distribution for $\theta_j^c = \{W_j^c, b_j^c\}$, which are the parameters of a linear readout layer used to solve the contrastive task. The rows of W_j^c thus correspond to class templates. Therefore, we use:

$$q(W_j^c; \tau, \sigma^2) = \mathcal{N}(\bar{W}_j^c, \sigma^2 I), \text{ with}$$

$$\bar{W}_j^c = \frac{1}{2\tau} \begin{bmatrix} - & f_{\theta^s}(\tilde{x}_1^A) + f_{\theta^s}(\tilde{x}_1^B) & - \\ & \vdots & \\ - & f_{\theta^s}(\tilde{x}_M^A) + f_{\theta^s}(\tilde{x}_M^B) & - \end{bmatrix}, \quad (3)$$

and neglect the biases b_j^c . In words, the mean representation of each pair of augmented images is used as the class template for each source image, which should solve the contrastive task well. The variational parameters τ and σ^2 , which determine the magnitude of the readout layer and the per-parameter variance, are shared across the contrastive tasks and are learnt by maximising Eq. (2) with reparameterisation gradients (Kingma & Welling, 2013). See Appendix B.2.1 for an ablation study on the effect of the pre-training approximate posterior.

Downstream Evaluation Having learnt a point estimate for θ^s , we can approximate the posterior over θ^t using any approximate inference technique.

Algorithm 1 summarises our approach. We found that using tempering with the mean-per-parameter KL divergence improved performance, in line with other work (e.g., Krishnan et al., 2022). Moreover, though our theory assumes a fixed set of contrastive task datasets, in practice, we generate a new \mathcal{D}_j^c per gradient step. Finally, following best-practice for contrastive learning (Chen et al., 2020a), we learn a non-linear *projection head* $g_\psi(\cdot)$ that is used *only* for the contrastive tasks. For further details, see Appendix A.

Understanding the Approximate Posterior To better understand $q(W_j^c; \tau, \sigma^2)$ (Eq. 3), we evaluate the likelihood term of Eq. (2) at the approximate posterior’s mean: \bar{W}_j^c . For convenience, define $\tilde{z}_i^A = f_{\theta^s}(\tilde{x}_i^A)$ and $\omega_i = (\tilde{z}_i^A + \tilde{z}_i^B)/2$, i.e., ω_i is the mean representation of the image pair produced by augmenting source image i . Then the log-likelihood $\log p(\mathcal{D}_j^c | \theta^s, \bar{W}_j^c)$ equals:

$$\sum_{i=1}^M \left[\log \frac{\exp \omega_i^T \tilde{z}_i^A / \tau}{\sum_{j=1}^M \exp \omega_j^T \tilde{z}_i^A / \tau} + \log \frac{\exp \omega_i^T \tilde{z}_i^B / \tau}{\sum_{j=1}^M \exp \omega_j^T \tilde{z}_i^B / \tau} \right].$$

Algorithm 1 Practical BSSL

Input: augmentations \mathcal{T} , unlabelled data \mathcal{D}^u , task data \mathcal{D}^t , contrastive prior $p(W^c)$

```

for  $j = 1, \dots, T$  do                                ▷ Contrastive pre-training
    Draw mini-batch  $\{x_i\}_{i=1}^M$ , set  $\mathcal{D}_j^c = \{\}$ 
    for  $i = 1, \dots, M$  do                                ▷ Form contrastive task
        Sample  $t^A, t^B \sim \mathcal{T}$ 
         $\tilde{x}_i^A = t^A(x_i), \tilde{x}_i^B = t^B(x_i)$ 
         $\tilde{z}_i^A = f_{\theta^s}(\tilde{x}_i^A), \tilde{z}_i^B = f_{\theta^s}(\tilde{x}_i^B)$ 
         $\omega_i = 0.5(\tilde{z}_i^A + \tilde{z}_i^B)$ 
         $\mathcal{D}_j^c = \mathcal{D}_j^c \cup \{(\tilde{x}_i^A, i)\} \cup \{(\tilde{x}_i^B, i)\}$ 
    end for
     $\tilde{W}_j^c = [\omega_1^T \dots \omega_M^T] / \tau + \epsilon$ , with  $\epsilon \sim \mathcal{N}(0, \sigma^2 I)$ 
     $\tilde{\mathcal{L}}(\tau, \sigma^2, \theta^s) = \log p(\theta^s) + \frac{1}{2M} p(\mathcal{D}_j^c | \theta^s, \tilde{W}_j^c)$ 
     $\quad - \bar{D}_{\text{KL}}[q(W_j^c) || p(W^c)]$ 
    Update  $\theta^s, \tau, \sigma^2$  to maximise  $\tilde{\mathcal{L}}(\tau, \sigma^2, \theta^s)$ 
end for
Approximate  $p(\theta^t | \mathcal{D}^t, \theta^s) \simeq q(\theta^t)$                 ▷ Downstream eval.
Predict using  $\mathbb{E}_{q(\theta^t)}[p(y_\star^t | x_\star, \theta^s, \theta^t)]$ 
    
```

We thus see that the above log-likelihood is a normalised-temperature cross-entropy loss (NT-XENT), as used by popular contrastive learning algorithms (Chen et al., 2020a;b). As such, not only can our practical BSSL algorithm be understood as an alternative contrastive learning approach, but standard contrastive learning algorithms can be interpreted as approaches for learning priors.

Comparison with SimCLR We saw that our objective function is similar to the NT-XENT loss, which is used by contrastive learning algorithms like SimCLR (Chen et al., 2020a), and is thus a contrastive pretraining algorithm with similar scalability and cost as SimCLR. We now discuss the differences between these approaches. First, in terms of learning the parameters of the base encoder, our objective: (i) is a principled lower bound for the (penalised) log-marginal likelihood, $p(\mathcal{D}_j^c | \theta^s)$; (ii) injects noise around \bar{W}^c , which may help regularise the base encoder (Srivastava et al., 2014); and (iii) has an adaptive temperature parameter τ that varies throughout training, which may be beneficial (Huang et al., 2022). Second, while contrastive learning typically uses the maximum likelihood to learn θ^t , we perform approximate Bayesian inference over these parameters.

BSSL as Type-II ML and Prior Learning As our objective function is a principled lower bound on the (penalised) log-marginal likelihood, it approximates type-II maximum likelihood (ML), which is often used to learn (hyper)parameters for deep kernels (Wilson et al., 2015) of Gaussian processes (Williams & Rasmussen, 2006), and recently also for BNNs (Immer et al., 2021). As such, similar to type-II ML, our approach can be understood as a form

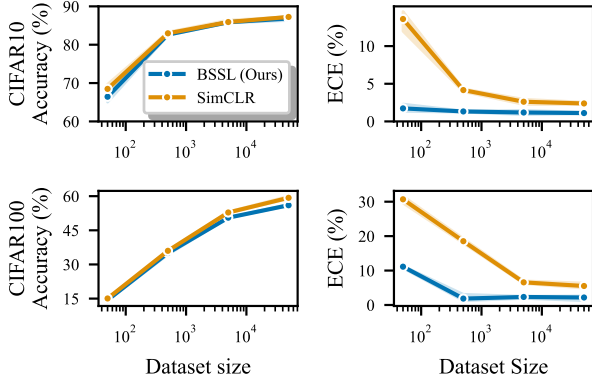


Figure 2: **Label efficiency of self-supervised learning approaches.** We compute the test accuracy and expected calibration error (ECE) when observing different numbers of labels of the CIFAR10 (top) and CIFAR100 (bottom) datasets. We compare SimCLR, a popular contrastive learning algorithm, to our BSSL approach, which uses the Laplace approximation for downstream evaluation and optimises a penalised evidence lower bound when training the base encoder. Mean and standard deviation across 3 seeds shown. We find BSSL is better calibrated than SimCLR.

of prior learning. Although we learn only a point-estimate for θ^s , this fixed value induces a prior distribution over predictive functions through the task-specific prior $p(\theta^t)$. However, while normal type-II ML learns this prior using the observed data itself, our approach maximises the marginal likelihood using the generated contrastive task datasets \mathcal{D}^c . As such, our approach *meta-learns* a prior predictive distribution using the generated contrastive datasets, similar to the use of the marginal likelihood in Bayesian meta-learning (Rothfuss et al., 2021). In §5, we show that this learnt prior predictive is well-suited for downstream tasks.

4. Comparison with SimCLR and BNNs

We now investigate the label efficiency of BSSL, a standard contrastive learning algorithm (SimCLR; Chen et al. 2020a), and BNN baselines on the CIFAR datasets. We consider a semi-supervised learning setup, which mimics the real-world scenario where there is an abundance of unlabelled data, but labelling datapoints is expensive or challenging. In particular, we show our approach is better calibrated than SimCLR and more label-efficient than BNNs, which together suggest BSSL learns an appropriate prior distribution for the downstream task and combines the benefits of BNNs and self-supervised learning.

Experiment Details We evaluate on CIFAR10 and CIFAR100, reserving a validation set of 1000 data points from the test set and using the remaining 9000 data points as the test set for evaluation. We evaluate the performance of

different baselines when conditioning on 50, 500, 5000, and 50000 labels. For BSSL and SimCLR, we use a ResNet-18 as the base encoder and include a non-linear projection head for contrastive pre-training, as is standard, and perform contrastive pre-training on the full train set. We use the data augmentations suggested by Chen et al. (2020a). We use a post-hoc Laplace approximation on the linear readout layer for BSSL downstream evaluation. For SimCLR, we evaluate using the linear evaluation protocol, which performs maximum likelihood on the linear readout layer. For the BNNs, we consider MAP, SWAG (Maddox et al., 2019), a deep ensemble (Lakshminarayanan et al., 2017), and last-layer Laplace (Daxberger et al., 2021), where again all networks use a ResNet-18 architecture. We chose these baselines because they are compatible with batch normalisation (Ioffe & Szegedy, 2015), which we use in the base architecture. See Appendix B.2 and B.3 for further details.

4.1. Comparison with Contrastive Learning

First, we compare the label efficiency of BSSL with SimCLR. Recall that, relative to SimCLR, our approach uses a modified pre-training objective that is a principled lower bound for the marginal likelihood. Further, our BSSL approach uses a Laplace approximation to make predictions.

We find that BSSL performs competitively with SimCLR at most dataset sizes in terms of accuracy, though it is slightly worse at some dataset sizes (Fig. 2). However, due to its principled Bayesian uncertainties, it is much better calibrated than SimCLR (in terms of expected calibration error, ECE), which we later see is useful for applications such as active learning (§6). Both approaches work well at low data regimes, suggesting that they provide effective mechanisms for learning prior predictive distributions.

To disentangle the effects of modifying the evaluation protocol and the pre-training objective, we run an ablation study (Appendix B.2.1). The Laplace evaluation protocol consistently improves performance with little overhead, so we recommend its use.

4.2. Comparison with BNNs

Second, we compare the label efficiency of BSSL with standard BNN baselines, a natural comparison as both approaches belong to the Bayesian deep learning framework.

We see that BSSL consistently outperforms the BNN baselines at low-to-medium data regimes (Fig. 3), even in terms of calibration, which suggests BSSL can learn a prior predictive that is suitable for this task. When conditioned on all labels, BSSL is outperformed in terms of accuracy by deep ensembles and SWAG, but has better-calibrated uncertainty estimates, even though these approaches use several trained networks for prediction and are thus employing sig-

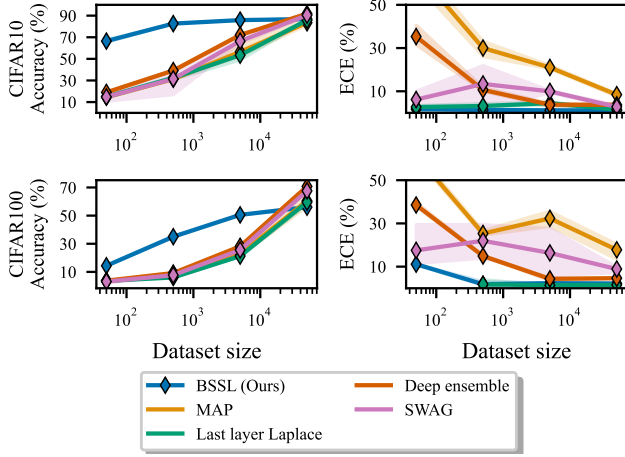


Figure 3: **Label efficiency of BNN approaches.** We compute the test accuracy and expected calibration error (ECE) for BSSL and BNN baselines when conditioning on different numbers of labels of the CIFAR10 (top) and CIFAR100 (bottom) datasets. Mean and standard deviation across 3 seeds shown. We see BSSL is more label efficient than the considered baselines.

nificantly more parameters than BSSL. Overall, BSSL yields well-calibrated uncertainty estimates and sample-efficiency, thereby combining the benefits of Bayesian methods and self-supervised learning.

5. BSSL Learns Suitable Prior Predictives

We saw that BSSL is more label-efficient than standard BNNs, suggesting that BSSL learns a prior predictive that is more suitable for downstream tasks than the BNN prior predictive. To test this hypothesis, we now investigate the prior predictive distributions of these methods. Such prior predictive checks are standard in the applied statistics community because they provide valuable information about model assumptions and generalisation (Gelman et al., 1995). However, they are challenging to apply to Bayesian neural networks because of the high-dimensional input space.

To overcome this difficulty, we rely on the following property. Intuitively, for an appropriate and informative prior, *the higher the semantic similarity between pairs of inputs, the more likely these inputs are to have the same label under the prior predictive*. We can therefore better understand a prior predictive distribution by also inspecting its behaviour for carefully chosen *pairs* of inputs, rather than by only inspecting its behaviour at single points in input space.

We consider the following pairs of images: (i) an image from the validation set (the “base image”) and an augmented version of the same image; (ii) a base image and another image of the same class; and (iii) a base image and an image of a different class. As these image pair groups have

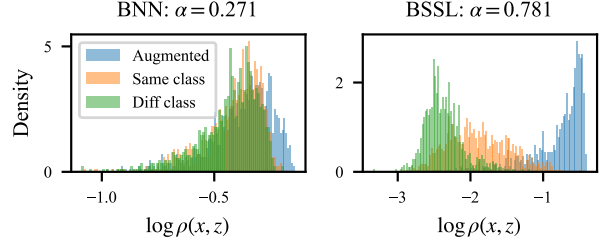


Figure 4: **BSSL and BNN Prior Predictives.** We assess the suitability of a prior predictive by computing the probability that particular pairs of images have the same label under the prior (ρ), and examining the distribution of ρ across different sets of image pairs that correspond to different levels of semantic similarity. We consider three sets: (i) augmented images; (ii) random images of the same class; and (iii) random images of different classes. Left: BNN prior. Right: prior learnt with BSSL. We see that the BSSL prior predictive captures the semantic similarity of the image pairs much better than the BNN prior, which is reflected in the prior evaluation score, α .

decreasing semantic similarity, we want the first group to be the most likely to have the same label, and the last group to be the least likely.

Experiment Details We investigate the different priors on CIFAR10. For the BNN, we follow Izmailov et al. (2021b) and use a ResNet-20-FRN with a $\mathcal{N}(0, 1/5)$ prior over network parameters and sample from the prior predictive. For the contrastive approaches, we train a base encoder of the same architecture and sample from the task prior predictive. For further details, see Appendix B.4.

Graphical Evaluation First, we visualise the BNN and BSSL prior predictives (Fig. 4). The BNN prior predictive assigns similar probabilities to all image pairs groups. In contrast, the BSSL prior has qualitatively different behaviour for each set of images, with the sets corresponding to higher semantic similarity being more likely to have the same label under the prior predictive. This suggests that the BSSL prior is much more suitable for the downstream classification task.

Quantitative Evaluation We now quantify the suitability of the prior predictive distribution. We define $\rho(x, z)$ as the probability that inputs x, z have the same label under the prior predictive, i.e., $\rho(x, z) = \mathbb{E}_{\theta}[p(y(x) = y(z)|\theta)]$ where $y(x)$ is the label corresponding to input x . Recall that for a suitable prior, the higher the semantic similarity between a pair of images, the higher ρ should be for that image pair. Therefore, to quantify the suitability of the prior predictive, we evaluate the frequency α under the data distribution that the ranking of ρ s that correspond to the aforementioned three sets of image pairs indeed match the

Table 1: Prior evaluation scores for different prior predictions on CIFAR10. Mean and standard deviation across three seeds shown. The contrastive (learnt) priors are much better than standard BNN priors.

Prior Predictive	Prior Score α
BNN — Gaussian	0.261 ± 0.024
BNN — Laplace	0.269 ± 0.007
SimCLR Prior	0.670 ± 0.015
BSSL Prior	0.680 ± 0.063

ranking of semantic similarities. Mathematically, we have:

$$\alpha = \mathbb{E}_{x, z_{1:3}} [\mathbb{I}(\underbrace{\rho(x, z_1)}_{\text{augmentation}} > \underbrace{\rho(x, z_2)}_{\text{same class}} > \underbrace{\rho(x, z_3)}_{\text{diff. class}})]$$

Each of the ρ -terms above corresponds to a different image pair group. In practice, we sample x from the underlying data distribution and then sample the corresponding z_i from the relevant group. The evaluation score, α , can be understood as a generalisation of the classic AUROC metric.

In Table 1, we see that the prior evaluation score for the BNN prior predictive is much lower than the learnt priors, in line with the graphical evaluation and our previous results (§4). Further, we find that standard SimCLR training *itself* learns a suitable prior distribution, which may partially explain the success of SimCLR. However, an approximate inference algorithm must also be used for well-calibrated uncertainty estimates (c.f., Fig. 2 and Appendix B.2.1).

6. BSSL Supports Label-Efficient Learning

We saw that BSSL offers better-calibrated uncertainty estimates than standard contrastive learning and better sample-efficiency than standard BNNs (§4), and learns a suitable prior predictive distribution (§5). We now demonstrate that BSSL supports label-efficient learning in two problem settings: semi-supervised learning and active learning.

6.1. Semi-Supervised Learning

We first consider a semi-supervised learning problem where we have all CIFAR10 training examples, but labels for only a fraction of those points. We compare: (i) supervised learning with a deep ensemble; (ii) unsupervised prior learning with BSSL and SimCLR, followed by supervised linear evaluation; and (iii) *semi-supervised prior learning* followed by supervised Laplace evaluation with BSSL.

Semi-Supervised Prior Learning By learning the base encoder’s parameters, θ^s , we effectively learn a suitable prior predictive for the downstream task. However, while we previously neglected the evidence \mathcal{D}^t provides about θ^s and only conditioned on the generated contrastive datasets, we will now additionally condition θ^s on \mathcal{D}^t . To do so, we

form a semi-supervised objective for θ^s , $\tilde{\mathcal{L}}_{ss}$ as:

$$\tilde{\mathcal{L}}(\theta^s) + \alpha (\mathbb{E}_{q(\theta^t)} [\log p(\mathcal{D}^t | \theta^t, \theta^s)] - \bar{D}_{KL}[q(\theta^t) || p(\theta^t)]),$$

where $\tilde{\mathcal{L}}$ is the standard BSSL objective, α controls the weighting between the task data and the contrastive data, and $q(\theta^t)$ is a variational distribution over the task specific-parameters. The above objective is a (reweighted) lower bound on the log-posterior density $p(\theta^s | \{\mathcal{D}_j^c\}, \mathcal{D}^t)$. See Appendix B.5 for further details.

Comparing these approaches (Fig. 5), we see that semi-supervised prior learning followed by Bayesian supervised evaluation performs best. Including labelled data during pre-training improves performance, and BSSL offers a principled approach to do so.

6.2. Active Learning

We now consider an active learning problem, where we assume we have access to a set of unlabelled examples and we want to carefully choose the data points to label.

Experiment Details We consider a low-budget active learning problem, which simulates a scenario where labelling is especially expensive. We use the CIFAR10 training set as the unlabelled pool set from which to label points. Further, we assume we are provided an initial training set of 50 randomly selected labelled points and a labelled validation set of the same size. We acquire 10 labels per acquisition round up to a maximum of 500 labels and evaluate using the full test set. We compare three models: BSSL, SimCLR, and a deep ensemble. Since BSSL and the deep ensemble provide epistemic uncertainty estimates, we use BALD (Houlsby et al., 2011) as the acquisition function. For SimCLR, we select points with the highest predictive entropy. We also consider uniform sampling for all methods. See Appendix B.6 for further details.

In Fig. 6, we see that BSSL using BALD selection achieves the highest accuracy across most numbers of labels permitted. Surprisingly, we see that uniform selection is a very strong baseline, with the active learning acquisition only boosting performance for BSSL—active learning *harms* the performance of SimCLR and the deep ensemble. The strong performance of BSSL, and the benefit of BALD over uniform sampling, provide further evidence for the principled uncertainty quantification of this approach (c.f., §4).

7. Related Work

Understanding and Improving Contrastive Learning Contrastive learning can be seen as an example of the InfoMax principle (Becker & Hinton, 1992), which maximises the mutual information between *representations* of two views of an input datum. Nevertheless, even though the

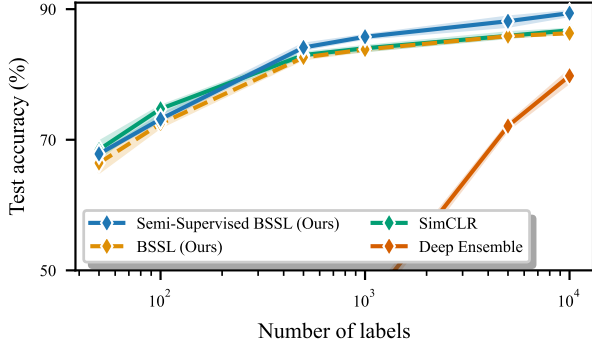


Figure 5: **Semi-supervised learning.** We consider semi-supervised learning on CIFAR10. All methods use the full training set, but only a fraction of the points have labels. We compare the test accuracy of: (i) a BSSL variant that includes labelled information during pre-training; (ii) BSSL with purely unsupervised pre-training; (iii) SimCLR; and (iv) a deep ensemble. Mean and standard deviation shown (3 seeds). We see that our method outperforms the baselines.

commonly used InfoNCE objective is a lower bound on this mutual information (Oord et al., 2019; Poole et al., 2019; Hénaff et al., 2020), this interpretation is at odds with empirical observations (Tschannen et al., 2020). Our framework, however, operates in *predictive* space—we aim to predict the source image index from an image, accounting for the architecture used for prediction. Others offer alternative interpretations of contrastive learning, from inverting the data-generating process (Zimmermann et al., 2022) to understanding InfoNCE as the objective of a self-supervised variational autoencoder (Aitchison, 2021). Conversely, we view contrastive pre-training as an effective means to learn suitable prior predictive distributions (§3.5). Finally, Sansone & Manhaeve (2022) develop a probabilistic interpretation of contrastive learning.

Learning Priors from Data We demonstrated BNNs have poor prior predictive distributions (§5), a concern also raised by others (e.g., Noci et al., 2021; Izmailov et al., 2021a; Fortuin et al., 2021; Wenzel et al., 2020). To improve BNN priors, some work *learns* priors, e.g., by using meta-learning (Garnelo et al., 2018; Rothfuss et al., 2021) or classic type-II maximum likelihood (Williams & Rasmussen, 2006; Wilson et al., 2015; Immer et al., 2021). We note that our framework is a form of meta-learning—the meta-training tasks are formed with data augmentation and mini-batching. Other approaches include the deep weight prior (Atanov et al., 2019), which trains a generative model over neural network weights as the prior. Standard data augmentation be seen as incorporating prior information and can also be used to learn a prior for a neural network (Nalisnick & Smyth, 2018). See Fortuin (2022) for an overview. Notably, Shwartz-Ziv et al. (2022) use transfer learning to specify informative BNN priors, considering SimCLR

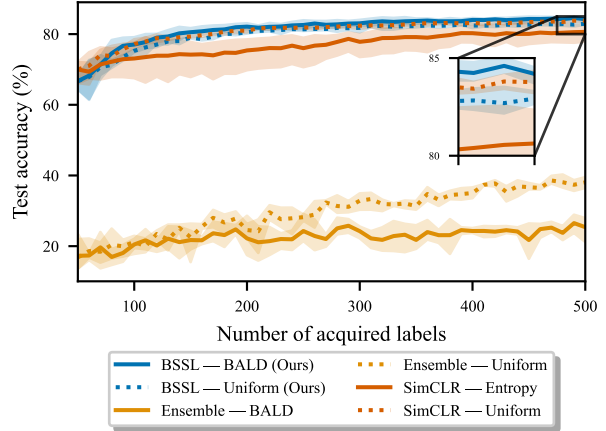


Figure 6: **Low-Budget Active Learning.** We consider active learning on CIFAR10 where we can label up to 1% of the training set. We compare: (i) BSSL; (ii) SimCLR; and (iii) a deep ensemble. For BSSL and the deep ensemble, we acquire points using the BALD metric, and we use predictive entropy for SimCLR. We further compare to uniform sampling for all methods. Mean and standard deviation shown (3 seeds). We see that BSSL outperforms all the baselines and that it is the only method for which active learning outperforms uniform sampling.

pre-training as a special case. In contrast, we propose a probabilistic model that enables unlabelled data to be accounted for within the Bayesian framework. Using this model, we derive a novel objective function that is a principled lower bound on a log-marginal likelihood for pre-training (§3). Further, we develop methodology that shows that contrastive pre-training *itself* learns a suitable prior predictive distribution (§5), and show how to perform *semi-supervised* prior learning (§6).

Deep Generative Models Deep generative models (DGMs) also leverage unlabelled data for improved downstream performance (Kingma & Welling, 2013; Kingma et al., 2014; Joy et al., 2020). DGMs generate supervision by reconstructing observed data from low-dimensional representations, i.e., they are *generative*. Our framework, however, is *discriminative*—supervision is through generated auxiliary labelled tasks. Both methods utilise unlabelled data to create auxiliary tasks, whether they be reconstructive or discriminative, but the nature of these tasks determine the practicality and performance of each method.

8. Discussion

To combine the sample-efficiency of self-supervised learning with the principles of Bayesian methods, we introduced a contrastive framework for Bayesian Self-Supervised Learning (BSSL; §3). Our framework enables BNNs to leverage unlabelled data, and our resulting practical al-

gorithm yields the sample-efficiency of self-supervised learning and the principled, well-calibrated uncertainties of Bayesian methods (§4). We interpret contrastive pre-training *itself*, whether with BSSL or SimCLR, as an effective mechanism for learning suitable prior predictive distributions (§5). Combining these prior predictive distributions with approximate inference schemes yields practical and performant algorithms that are no less principled than conventional BNNs and naturally support data-efficient learning (§6). We strongly recommend the use of contrastive pre-training with approximate inference for downstream tasks, and are excited to see future work that uses BSSL to learn richer prior distributions.

ACKNOWLEDGEMENTS

MS was supported by the EPSRC Centre for Doctoral Training in Autonomous Intelligent Machines and Systems (EP/S024050/1), and thanks Rob Burbea for inspiration and support. VF was supported by a Postdoc Mobility Fellowship from the Swiss National Science Foundation, a Research Fellowship from St John’s College Cambridge, and a Branco Weiss Fellowship.

References

- Aitchison, L. InfoNCE is a variational autoencoder, July 2021. URL <http://arxiv.org/abs/2107.02495>. arXiv:2107.02495 [cs, stat].
- Atanov, A., Ashukha, A., Struminsky, K., Vetrov, D., and Welling, M. The Deep Weight Prior. *arXiv:1810.06943 [cs, stat]*, February 2019. URL <http://arxiv.org/abs/1810.06943>. arXiv: 1810.06943.
- Becker, S. and Hinton, G. E. Self-organizing neural network that discovers surfaces in random-dot stereograms. *Nature*, 355(6356):161–163, January 1992. ISSN 1476-4687. doi: 10.1038/355161a0. URL <https://www.nature.com/articles/355161a0>. Number: 6356 Publisher: Nature Publishing Group.
- Blundell, C., Cornebise, J., Kavukcuoglu, K., and Wierstra, D. Weight uncertainty in neural network. In *International conference on machine learning*, pp. 1613–1622. PMLR, 2015.
- Chen, T., Kornblith, S., Norouzi, M., and Hinton, G. A Simple Framework for Contrastive Learning of Visual Representations. *arXiv:2002.05709 [cs, stat]*, June 2020a. URL <http://arxiv.org/abs/2002.05709>. arXiv: 2002.05709.
- Chen, T., Kornblith, S., Swersky, K., Norouzi, M., and Hinton, G. Big Self-Supervised Models are Strong Semi-Supervised Learners. *arXiv:2006.10029 [cs, stat]*, October 2020b. URL <http://arxiv.org/abs/2006.10029>. arXiv: 2006.10029.
- Chen, X. and He, K. Exploring Simple Siamese Representation Learning, November 2020. URL <http://arxiv.org/abs/2011.10566>. arXiv:2011.10566 [cs].
- D’Angelo, F. and Fortuin, V. Repulsive deep ensembles are bayesian. *Advances in Neural Information Processing Systems*, 34:3451–3465, 2021.
- Daxberger, E., Kristiadi, A., Immer, A., Eschenhagen, R., Bauer, M., and Hennig, P. Laplace redux-effortless bayesian deep learning. *Advances in Neural Information Processing Systems*, 34:20089–20103, 2021.
- Fortuin, V. Priors in bayesian deep learning: A review. *International Statistical Review*, 2022.
- Fortuin, V., Garriga-Alonso, A., Wenzel, F., Rätsch, G., Turner, R., van der Wilk, M., and Aitchison, L. Bayesian Neural Network Priors Revisited. *arXiv:2102.06571 [cs, stat]*, February 2021. URL <http://arxiv.org/abs/2102.06571>. arXiv: 2102.06571.
- Gal, Y., Islam, R., and Ghahramani, Z. Deep bayesian active learning with image data. In *International Conference on Machine Learning*, pp. 1183–1192. PMLR, 2017.
- Garnelo, M., Schwarz, J., Rosenbaum, D., Viola, F., Rezende, D. J., Eslami, S. M. A., and Teh, Y. W. Neural Processes, July 2018. URL <http://arxiv.org/abs/1807.01622>. arXiv:1807.01622 [cs, stat].
- Gelman, A., Carlin, J. B., Stern, H. S., and Rubin, D. B. *Bayesian data analysis*. Chapman and Hall/CRC, 1995.
- Grill, J.-B., Strub, F., Altché, F., Tallec, C., Richemond, P. H., Buchatskaya, E., Doersch, C., Pires, B. A., Guo, Z. D., Azar, M. G., Piot, B., Kavukcuoglu, K., Munos, R., and Valko, M. Bootstrap your own latent: A new approach to self-supervised Learning, September 2020. URL <http://arxiv.org/abs/2006.07733>. arXiv:2006.07733 [cs, stat].
- He, K., Fan, H., Wu, Y., Xie, S., and Girshick, R. Momentum contrast for unsupervised visual representation learning. In *Proceedings of the IEEE/CVF conference on computer vision and pattern recognition*, pp. 9729–9738, 2020.
- Houlsby, N., Huszár, F., Ghahramani, Z., and Lengyel, M. Bayesian active learning for classification and preference learning. *arXiv preprint arXiv:1112.5745*, 2011.
- Huang, Z., Zhang, C., Li, H., Wang, B., and Chen, C. Model-Aware Contrastive Learning: Towards Escaping Uniformity-Tolerance Dilemma in Training, August 2022. URL <http://arxiv.org/abs/2207.07874>. arXiv:2207.07874 [cs].

- Hénaff, O. J., Srinivas, A., De Fauw, J., Razavi, A., Doersch, C., Eslami, S. M. A., and Oord, A. v. d. Data-Efficient Image Recognition with Contrastive Predictive Coding, July 2020. URL <http://arxiv.org/abs/1905.09272>. arXiv:1905.09272 [cs].
- Immer, A., Bauer, M., Fortuin, V., Rätsch, G., and Emtiyaz, K. M. Scalable marginal likelihood estimation for model selection in deep learning. In *International Conference on Machine Learning*, pp. 4563–4573. PMLR, 2021.
- Ioffe, S. and Szegedy, C. Batch normalization: Accelerating deep network training by reducing internal covariate shift. In *International conference on machine learning*, pp. 448–456. PMLR, 2015.
- Izmailov, P., Nicholson, P., Lotfi, S., and Wilson, A. G. Dangers of Bayesian Model Averaging under Covariate Shift. *arXiv:2106.11905 [cs, stat]*, June 2021a. URL <http://arxiv.org/abs/2106.11905>. arXiv:2106.11905.
- Izmailov, P., Vikram, S., Hoffman, M. D., and Wilson, A. G. What Are Bayesian Neural Network Posteriors Really Like? *arXiv:2104.14421 [cs, stat]*, April 2021b. URL <http://arxiv.org/abs/2104.14421>. arXiv:2104.14421.
- Joy, T., Schmon, S. M., Torr, P. H., Siddharth, N., and Rainforth, T. Capturing label characteristics in vaes. *arXiv preprint arXiv:2006.10102*, 2020.
- Kingma, D. P. and Welling, M. Auto-encoding variational bayes. *arXiv preprint arXiv:1312.6114*, 2013.
- Kingma, D. P., Rezende, D. J., Mohamed, S., and Welling, M. Semi-Supervised Learning with Deep Generative Models, October 2014. URL <http://arxiv.org/abs/1406.5298>. arXiv:1406.5298 [cs, stat].
- Kingma, D. P., Salimans, T., and Welling, M. Variational dropout and the local reparameterization trick. *Advances in neural information processing systems*, 28, 2015.
- Krishnan, R., Esposito, P., and Subedar, M. Bayesian-Torch: Bayesian neural network layers for uncertainty estimation, January 2022. URL <https://github.com/IntelLabs/bayesian-torch>.
- Lakshminarayanan, B., Pritzel, A., and Blundell, C. Simple and scalable predictive uncertainty estimation using deep ensembles. *Advances in neural information processing systems*, 30, 2017.
- Loshchilov, I. and Hutter, F. Decoupled weight decay regularization. *arXiv preprint arXiv:1711.05101*, 2017.
- Mackay, D. J. C. Bayesian Methods for Adaptive Models. Technical report, 1992.
- Maddox, W. J., Izmailov, P., Garipov, T., Vetrov, D. P., and Wilson, A. G. A simple baseline for bayesian uncertainty in deep learning. *Advances in Neural Information Processing Systems*, 32, 2019.
- Nalisnick, E. and Smyth, P. Learning Priors for Invariance. In *International Conference on Artificial Intelligence and Statistics*, pp. 366–375. PMLR, March 2018. URL <http://proceedings.mlr.press/v84/nalisnick18a.html>. ISSN: 2640-3498.
- Nalisnick, E. T. *On priors for Bayesian neural networks*. University of California, Irvine, 2018.
- Neal, R. M. BAYESIAN LEARNING FOR NEURAL NETWORKS. Technical report, 1995.
- Noci, L., Roth, K., Bachmann, G., Nowozin, S., and Hofmann, T. Disentangling the Roles of Curation, Data-Augmentation and the Prior in the Cold Posterior Effect. *arXiv:2106.06596 [cs]*, June 2021. URL <http://arxiv.org/abs/2106.06596>. arXiv:2106.06596.
- Oord, A. v. d., Li, Y., and Vinyals, O. Representation Learning with Contrastive Predictive Coding, January 2019. URL <http://arxiv.org/abs/1807.03748>. arXiv:1807.03748 [cs, stat].
- Ovadia, Y., Fertig, E., Ren, J., Nado, Z., Sculley, D., Nowozin, S., Dillon, J., Lakshminarayanan, B., and Snoek, J. Can you trust your model’s uncertainty? evaluating predictive uncertainty under dataset shift. *Advances in neural information processing systems*, 32, 2019.
- Poole, B., Ozair, S., Oord, A. v. d., Alemi, A. A., and Tucker, G. On Variational Bounds of Mutual Information, May 2019. URL <http://arxiv.org/abs/1905.06922>. arXiv:1905.06922 [cs, stat].
- Rothfuss, J., Fortuin, V., Josifoski, M., and Krause, A. Pachoh: Bayes-optimal meta-learning with pac-guarantees. In *International Conference on Machine Learning*, pp. 9116–9126. PMLR, 2021.
- Sansone, E. and Manhaeve, R. Gedi: Generative and discriminative training for self-supervised learning. *arXiv preprint arXiv:2212.13425*, 2022.
- Sharma, M., Farquhar, S., Nalisnick, E., and Rainforth, T. Do Bayesian Neural Networks Need To Be Fully Stochastic?, November 2022. URL <http://arxiv.org/abs/2211.06291>. arXiv:2211.06291 [cs, stat].
- Shwartz-Ziv, R., Goldblum, M., Souri, H., Kapoor, S., Zhu, C., LeCun, Y., and Wilson, A. G. Pre-Train Your Loss: Easy Bayesian Transfer Learning with Informative Priors, May 2022. URL <http://arxiv.org/abs/2205.10279>. arXiv:2205.10279 [cs].

Srivastava, N., Hinton, G., Krizhevsky, A., Sutskever, I., and Salakhutdinov, R. Dropout: A Simple Way to Prevent Neural Networks from Overfitting. *Journal of Machine Learning Research*, 15(56):1929–1958, 2014. ISSN 1533-7928. URL <http://jmlr.org/papers/v15/srivastava14a.html>.

Tran, B.-H., Rossi, S., Milios, D., and Filippone, M. All you need is a good functional prior for bayesian deep learning. *arXiv preprint arXiv:2011.12829*, 2020.

Tschannen, M., Djolonga, J., Rubenstein, P. K., Gelly, S., and Lucic, M. On Mutual Information Maximization for Representation Learning, January 2020. URL <http://arxiv.org/abs/1907.13625>. arXiv:1907.13625 [cs, stat].

Welling, M. and Teh, Y. W. Bayesian learning via stochastic gradient langevin dynamics. In *Proceedings of the 28th international conference on machine learning (ICML-11)*, pp. 681–688, 2011.

Wen, Y., Vicol, P., Ba, J., Tran, D., and Grosse, R. Flipout: Efficient pseudo-independent weight perturbations on mini-batches. *arXiv preprint arXiv:1803.04386*, 2018.

Wenzel, F., Roth, K., Veeling, B. S., Swiatkowski, J., Tran, L., Mandt, S., Snoek, J., Salimans, T., Jenatton, R., and Nowozin, S. How Good is the Bayes Posterior in Deep Neural Networks Really? *arXiv*, February 2020. URL <http://arxiv.org/abs/2002.02405>. Publisher: arXiv.

Williams, C. K. and Rasmussen, C. E. *Gaussian processes for machine learning*, volume 2. MIT press Cambridge, MA, 2006.

Wilson, A. G. and Izmailov, P. Bayesian deep learning and a probabilistic perspective of generalization. *Advances in neural information processing systems*, 33:4697–4708, 2020.

Wilson, A. G., Hu, Z., Salakhutdinov, R., and Xing, E. P. Deep Kernel Learning, November 2015. URL <http://arxiv.org/abs/1511.02222>. arXiv:1511.02222 [cs, stat].

You, Y., Gitman, I., and Ginsburg, B. Scaling sgd batch size to 32k for imagenet training. *arXiv preprint arXiv:1708.03888*, 6(12):6, 2017.

Zimmermann, R. S., Sharma, Y., Schneider, S., Bethge, M., and Brendel, W. Contrastive Learning Inverts the Data Generating Process, April 2022. URL <http://arxiv.org/abs/2102.08850>. arXiv:2102.08850 [cs].

A. Practical Considerations

In §3, we derived a contrastive framework for Bayesian Self-Supervised Learning (BSSL), which we then used to develop a practical algorithm (Algorithm 1). We now provide some additional further details used for our practical method.

To recap our framework, we use data augmentation and mini-batching to create a set of contrastive tasks $\{\mathcal{D}^c\}$. Further employing parameter sharing between the labels of each \mathcal{D}^c and the labels of \mathcal{D}^t allows us to condition on \mathcal{D}^c when making predictions on \mathcal{D}^t , thereby improving downstream predictions.

In practice, we share parameters θ^s across all tasks (i.e., across the generated contrastive tasks and the actual downstream task), and learn a θ^t separately for each task. We focus on image classification problems and let θ^s be the parameters of a *base encoder*, which produces a representation z . θ^t are the parameters of a linear readout layer that makes predictions from z . In §3, we discussed learning a point-estimate for θ^s by maximising the penalised evidence lower bound:

$$\tilde{\mathcal{L}}(\theta^s) = \log p(\theta^s) + \sum_j \mathbb{E}_{q(\theta_j^t)} [\log p(\mathcal{D}_j^c | \theta_j^t, \theta^s) - D_{\text{KL}}(q(\theta_j^t) || p(\theta^t))]. \quad (4)$$

For our practical algorithm, we make a number of changes relative to this objective function because they follow best-practice, either in the contrastive learning or Bayesian deep learning community, and improve performance.

1. We add a non-linear projection head to the base encoder architecture *only for the contrastive task datasets*. As such, we use $z = g_\phi(f_{\theta^s}(x)) / \|g_\phi(f_{\theta^s}(x))\|$ for \mathcal{D}^c . $g_\phi(\cdot)$ is the projection head, and the representation is normalised. For the downstream tasks, we use $z = f_{\theta^s}(x)$, i.e., we “throw-away” the projection head. This is best practice within the contrastive learning community (Chen et al., 2020a;b).
2. We *temper* the KL divergence term, using the mean-per-parameter KL divergence (denoted as $\bar{D}_{\text{KL}}(\cdot || \cdot)$). Tempering is necessary for several Bayesian deep learning algorithms to perform well (Wenzel et al., 2020; Krishnan et al., 2022).
3. Rather than generating a fixed set of contrastive task datasets, $\{\mathcal{D}^c\}$, and optimising Eq. (4), we generate a new contrastive task dataset per gradient step, perform one gradient update step on that dataset, and then discard that dataset. This follows standard contrastive learning algorithms (Chen et al., 2020a). Moreover, we rescale each $\log p(\mathcal{D}_j^c | \theta_j^t, \theta^s)$ term in Eq. (4) to be $\frac{1}{|\mathcal{D}_j^c|} \log p(\mathcal{D}_j^c | \theta_j^t, \theta^s)$, i.e., we use the *average* log-likelihood, not the total log-likelihood, and instead of having an explicit prior distribution over θ^s , we use standard weight-decay for training i.e., we specify a penalty on the norm of the weights of the encoder *per gradient step*.

Together, these changes yield the objective function used in Algorithm 1. Finally, we note that different practical algorithms ensue depending on the choice of θ^t , the choice of θ^s , and the techniques used to perform approximate inference. We employ variational inference and learn a point estimate for θ^s , but there are other choices. For instance, employing SWAG inference to learn θ^s (Maddox et al., 2019) would yield an approach similar to Pre-train Your Loss (Shwartz-Ziv et al., 2022). We are excited to see future work that utilises our framework in different ways to learn rich prior predictive distributions.

B. Additional Results and Experiment Details

We now provide further experiment details and additional results. Unless otherwise mentioned, details for BSSL follow the details provided in §B.1

B.1. BSSL

B.1.1. CONTRASTIVE PRE-TRAINING

Base Architecture We use a ResNet-18 architecture, modified for the size of CIFAR10 images, following Chen et al. (2020a). The representations produced by this architecture have dimensionality 512. Further, for the non-linear projection head, we use a 2 layer multi-layer perceptron (MLP) with output dimensionality 128.

Contrastive Augmentations We follow Chen et al. (2020a) and compose a random resized crop, a random horizontal flip, random colour jitter, and random grayscale for the augmentation. These augmentations make up the contrastive augmentation set \mathcal{T} . We finally normalise the images to have mean 0 and standard deviation 1 per channel, as is standard.

Hyperparameters We use a $\mathcal{N}(0, \frac{1}{\tau_p})$ prior over the linear parameters θ^t , and tune τ_p for each dataset. As such, τ can be understood as the prior temperature. We use $\tau_p = 0.65$ for CIFAR10 and $\tau_p = 0.6$ for CIFAR100. We use weight decay $1e - 6$ for the base encoder and projection head parameters.

Variational Distribution We parameterize the temperature and noise scale using the log of their values. That is, we have $\sigma = \exp \tilde{\sigma}$.

Optimisation Details We use the LARS optimiser (You et al., 2017), with batch size 1000 and momentum 0.9. We train for 500 epochs, using a linear warmup cosine annealing learning rate schedule. The warmup starting learning rate for the base encoder parameters is $1e - 3$ with a maximum learning rate of 0.6. For the variational parameters, the maximum learning rate is $1e - 3$, which we found to be important for the stability of the algorithm.

B.1.2. EVALUATION

Having trained a base encoder, we perform approximate inference for the task-specific linear layer parameters θ^t using the post-hoc Laplace approximation, implemented the Laplace library (Daxberger et al., 2021). This inference method first trains a point-estimate for θ^t which is used as the mean of the approximate posterior. To estimate the covariance of the approximate posterior, the Hessian is approximated.

Linear Evaluation Protocol To train the point estimate needed for Laplace’s method, we use the linear evaluation protocol. We update the last-layer linear readout parameters using the AdamW (Loshchilov & Hutter, 2017) optimiser with batch size 1000, no weight decay and learning rate 10^{-2} . We train for a maximum of 300 epochs, but terminate training if the validation loss has not improved for 10 epochs. We use the checkpoint with the highest validation accuracy. We additionally use random resized crops and random horizontal flips as data augmentation that boosts the performance of the linear evaluation.

Laplace Evaluation Protocol With a point estimate for θ^t found using the linear evaluation protocol, we apply the post-hoc Laplace approximation using the generalised Gauss-Newton approximation to the Hessian. For CIFAR10, we use a full covariance approximation and for CIFAR100 we use a Kronecker-factorised approximation for the Hessian of the last layer weights and biases. We tune the prior precision by maximising the likelihood of a validation set. For predictions, we use the (extended) probit approximation. These choices follow recommendations from Daxberger et al. (2021).

B.2. Comparison with Contrastive Learning (§4.1)

Experiment Setup For these experiments, we use the entire training set for contrastive pre-training. We then perform supervised linear/Laplace evaluation on varying numbers of labels from the train set. For the evaluation protocols, we reserve a validation set of 1000 data points from the test set and evaluate using the remaining 9000 labels.

SimCLR For SimCLR (Chen et al., 2020a), we use primarily use the same hyperparameters as for BSSL, except that we separately tune the temperature parameter. We use $\tau = 0.45$ for CIFAR10 and $\tau = 0.3$ for CIFAR100, selected by maximising the average log-likelihood across multiple data sizes. For evaluation, we use only the linear evaluation protocol. See Appendix B.1 for more details.

B.2.1. ABLATION STUDIES

Effect of Pre-training Objective and Evaluation Method Recall that our practical BSSL algorithm is reminiscent of SimCLR, but uses a modified objective function that is a principled lower bound of the log-marginal likelihood to learn the base-encoder parameters, and performs approximate inference on the task-specific parameters θ^t .

To better disentangle the effects of the modified pretraining objective and the modified evaluation method, we ran an ablation study (Fig. 7). We find performing approximate inference for downstream evaluation substantially improves calibration, and therefore strongly recommend its use. In contrast, both pretraining objectives (with Laplace) evaluation perform similarly at most dataset sizes, except for the smallest datasets sizes where SimCLR pre-training performs slightly better.

Effect of Batch Size We study the effect of the pre-training batch size on the performance of our BSSL approach. We run one seed for 100 epochs across three different batch sizes on CIFAR10. We see in Table 2, the performance on CIFAR10 is

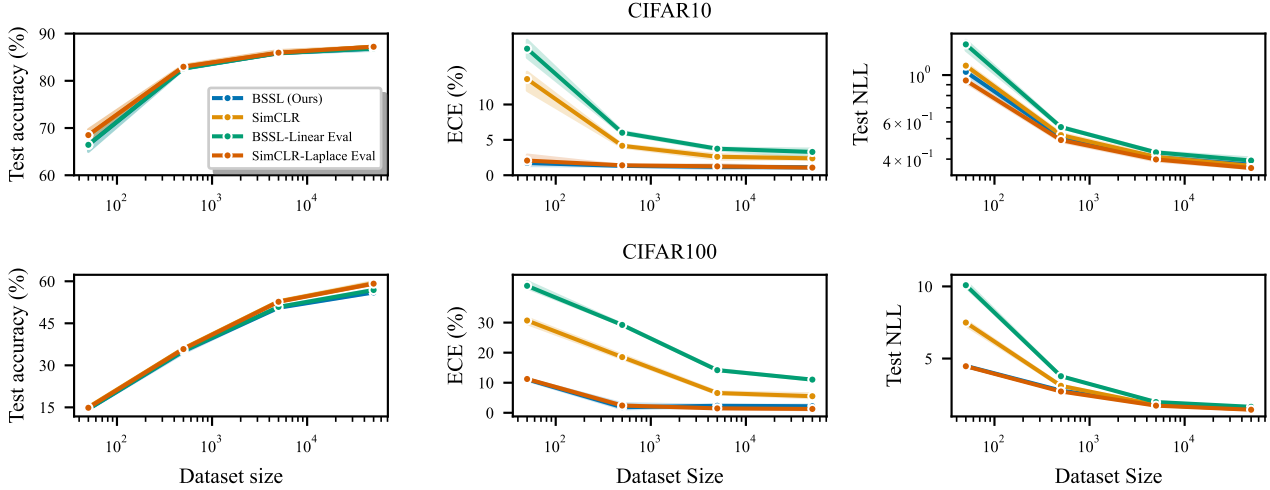


Figure 7: **Self-supervised learning ablation study.** We compute the test accuracy, expected calibration error (ECE) and negative log-likelihood when observing different numbers of labels of the CIFAR10 (top) and CIFAR100 (bottom) datasets. We consider: (i) BSSL pre-training and Laplace downstream evaluation (BSSL); (ii) SimCLR pre-training and maximum likelihood evaluation (SimCLR); (iii) BSSL pre-training and maximum likelihood evaluation (BSSL-Linear Eval); and (iv) SimCLR with Laplace evaluation (SimCLR-Laplace Eval). Mean and standard deviation across 3 seeds are shown.

robust to reducing the batch size. We hypothesise this is due to the noise injected during pre-training.

Table 2: Effect of pretraining batch size on BSSL performance on CIFAR10.

Batch Size	CIFAR10 Accuracy (%)
100	0.81
500	0.81
1000	0.80

Effect of Variational Distribution We run an ablation study changing the variational distribution mean on CIFAR10. We evaluation using one seed, training for 100 epochs only. We consider setting the mean of the variational distribution for image i , ω_i , to be: $0.5(\tilde{z}_i^A + \tilde{z}_i^B)$, \tilde{z}_i^A , and $\mathbf{0}$. We see a suitable mean is required for good performance.

Table 3: Effect of pretraining variational distribution mean on BSSL performance on CIFAR10.

Variational Distribution Mean	CIFAR10 Accuracy (%)
$\mathbf{0}$	0.19
\tilde{z}_i^A	0.79
$0.5(\tilde{z}_i^A + \tilde{z}_i^B)$	0.80

B.3. Comparison with BNNs (§4.2)

The experiment setup here follows Appendix B.2. Here, we focus on providing details for the BNN baselines. All baselines use the same ResNet-18 architecture, which was modified for the image size used in the CIFAR image datasets. The baselines we considered were chosen because they are all compatible with batch normalisation, which is included in the base architecture. We provide further details about the baselines below.

MAP For the maximum-a-posterior network, we use the Adam optimiser with learning rate 10^{-3} , default weight decay, and batch size 1000. We train for a minimum of 25 epochs and a maximum of 300 epochs, terminating training early if the validation loss increases for 3 epochs in a row.

Last-Layer Laplace For the Last-Layer Laplace baseline, we perform a post-hoc Laplace approximation to a MAP network trained using the protocol above. We use the same settings as for BSSL Laplace evaluation, see Appendix B.1.

Deep Ensemble For the deep ensemble baseline, we train 5 MAP networks starting from different initialisations using the above protocol, and aggregate their predictions.

SWAG For the SWAG baseline, we first a MAP network using the above protocol. We then run SGD from this solution for 10 epochs, taking 4 snapshots per epoch, and using $K = 20$ as the rank of the covariance matrix. We choose the SWAG learning rate per run using the validation set, and consider 10^{-2} , 10^{-3} , and 10^{-4} .

B.4. Prior Predictive Checks (§5)

BNN Prior Predictive We use the ResNet-20-FRN architecture, which is the architecture used by Izmailov et al. (2021b). Note that this architecture does not include batch normalisation, which means the prior over parameters straightforwardly corresponds to a prior predictive distribution. We use a $\mathcal{N}(0, \frac{1}{5})$ prior over all network weights, again following Izmailov et al. (2021b), and sample from the prior predictive using 8192 Monte Carlo samples.

Contrastive Prior Predictives We primarily follow the details outlined earlier (Appendix B.1), except we use the same ResNet-20-FRN architecture as used for the BNNs and we use a batch size of 500 rather than 1000. To sample from the prior predictive, we use $y \sim \text{softmax}(W f_{\theta^s}(x))$, where we normalise the representations produced by the base encoder to have zero mean and unit variance, and we have $W \sim \mathcal{N}(0, 20)$, with the prior precision chosen by hand. The prior evaluation scores are not sensitive to the prior score choice, and are evaluated by sampling images from the validation set, which was not seen during training. We used 4096 Monte Carlo samples from the prior. Since contrastive pre-training has access to the CIFAR10 train set, we evaluate on the validation set, which was not seen during training.

B.5. Semi-Supervised Learning (§6.1)

The details used for the BNN baseline, SimCLR, and the unsupervised BSSL variant follow the earlier sections in the appendix. For the semi-supervised BSSL variant, we include an additional term in the objective function:

$$\tilde{\mathcal{L}}_{\text{ss}}(\theta^s) = \tilde{\mathcal{L}}(\theta^s) + \alpha[\mathbb{E}_{q_\phi(\theta^t)}[\log p(\mathcal{D}^t | \theta^s, \theta^t)] - \beta D_{\text{KL}}[q_\phi(\theta^t) || p(\theta^t)]], \quad (5)$$

i.e., we introduce a variational distribution on the task parameters. This is used to provide a lower bound on the evidence provided by \mathcal{D}^t on θ^s . We use mean-field variational inference over θ^t with a Gaussian approximate posterior and Flipout (Wen et al., 2018). We use the implementation from Krishnan et al. (2022), and temper by setting $\beta = 1/|\theta^t|$, meaning we use the average per-parameter KL divergence. α is a hyperparameter that controls the relative weighting between the generated contrastive task datasets and the observed label data, and is tuned. We use $\alpha = 5 \cdot 10^{-5}$ when we have fewer than 100 labels, and $\alpha = 5 \cdot 10^{-3}$ otherwise. For $p(\theta^t)$, we use a $\mathcal{N}(0, 1)$ prior. For downstream evaluation, we use the Laplace evaluation protocol. For this experiment, we use only the CIFAR10 dataset.

B.6. Active Learning (§6.2)

We simulate a low-budget active learning setting. For each method, we use their default implementation details as outlined in this Appendix. With regards to the active learning setup, we assume that we have access to a small validation set of 50 labelled examples and are provided 50 labelled training examples. We acquire 10 examples per acquisition round up to a maximum of 500 labelled examples, which corresponds to 1% of the labels in the training set. We evaluate using the full test set. For all methods (the deep ensemble, SimCLR, and BSSL), we consider uniform sampling. The deep ensemble and BSSL provide epistemic uncertainty estimates, so we perform active learning by selecting the points with the highest BALD metric (Houlsby et al., 2011). For SimCLR, we acquire points using the highest predictive entropy, a commonly used baseline (Gal et al., 2017). For this experiment, we use only the CIFAR10 dataset.